Second Sound Attenuation in Liquid Helium II

W. B. HANSON*† AND J. R. PELLAM‡
National Bureau of Standards, Washington, D. C.
(Received April 1, 1954)

Second sound attenuation was measured in the hundred kilocycle per second frequency range with a continuous wave method. Measurements were carried out over the temperature interval from 1.25°K to 2.17°K. The short wavelengths employed and the absence of walls near the second sound beam caused geometrical attenuation and wall losses to be negligible compared to the actual liquid attenuation.

The attenuation was found to be amplitude independent for the small amplitudes employed. The expected increase of attenuation with the square of the frequency was experimentally verified up to 0.27 Mc/sec. Excellent agreement with Khalatnikov's latest theory was obtained for both the magnitude and temperature dependence of the attenuation. The attenuation was found to increase rapidly as the λ point was approached and apparently becomes infinite there.

I. INTRODUCTION

THE phenomenon of second sound propagation in liquid helium II is well known. Early theoretical[1,2] and experimental[3,4] investigations demonstrated the anomalous heat flow characteristics of helium II and showed that the ordinary heat conduction equation does not apply. Instead a true reversible wave equation is involved, and the resulting thermal propagation displays the usual characteristics of true wave behavior.

The first-order properties of these thermal waves, called second sound, have been studied intensively since their discovery by Peshkov in 1946. Thus the velocity behavior has been determined reliably from the λ point (2.19°K) down to about 0.5°K and has been observed down to temperatures of the order of 0.01°K. Although until recently no serious attempts have been made to measure such second-order properties of these waves as attenuation, this quantity has been under consideration from the theoretical standpoint for some time. Experimental developments have now progressed to the point where reliable attenuation measurements can be achieved, and the purpose of the present investigation was to measure this absorption as a function of frequency and temperature.

The subject of second sound attenuation has been examined by several authors. The *temperature amplitude attenuation coefficient* α under consideration is defined by the relationship

$$\tau(x)=\tau(0)e^{-\alpha x} \tag{1}$$

for plane wave propagation, where $\tau(x)$ is the temperature deviation from the ambient as a function of distance x. The contribution to attenuation attributable to the ordinary viscosity of the normal fluid component was given in 1948 by Pellam[5] as

$$\alpha_{\text{vis}(1)}=\frac{2}{3}\frac{\omega^2}{\rho v_2^3}\frac{\rho_s}{\rho_n}\eta, \tag{2}$$

in terms of the angular frequency ω ($\omega=2\pi\nu$), the wave velocity of second sound v_2, and the component densities ρ_n and ρ_s of normal fluid and superfluid. Since the coefficient of ordinary viscosity η of normal fluid has since been termed "first viscosity" by Khalatnikov,[6] the above contribution to the attenuation coefficient is indicated by the subscript vis(1).

As has been recently shown by Khalatnikov, two additional processes contribute to the attenuation of second sound in liquid helium II. The presence of these additional mechanisms became apparent to Khalatnikov in connection with his analysis of earlier observations of *first sound* attenuation in liquid helium II. In 1947 Pellam and Squire[7] had measured the absorption of ordinary (first) sound in liquid helium II and found not only an anomalously high value of attenuation, but also an *increase* with decreasing temperature. Although Andronikashvilli's 1948 viscosity measurements could explain the above-mentioned temperature dependence of the first sound absorption, the complete disagreement in actual order of magnitude was interpreted by Khalatnikov as evidence of complicated dynamic interactions not involved in the ordinary viscosity.

Khalatnikov was able to explain this excessive first sound absorption in terms of a new viscous process associated with both normal fluid and superfluid which he called "second viscosity." He showed that this second viscosity should be the predominant factor in first sound absorption below 2.0°K and that the absorption should continue to increase as the temperature was lowered. This was later verified by Atkins and

* Submitted in partial fulfillment of the requirements for the degree of Doctor of Philosophy at the George Washington University.

† Now at the N.B.S. Cryogenic Engineering Laboratory, Boulder, Colorado.

‡ Now at California Institute of Technology, Pasadena, California.

[1] L. Tisza, Compt. rend. **207**, 1035, 1186 (1938).

[2] E. M. Lifshitz, J. Phys. (U.S.S.R.) **8**, 110 (1944).

[3] V. P. Peshkov, J. Exptl. Theoret. Phys. (U.S.S.R.) **10**, 389 (1946).

[4] Keesom, Saris, and Meyer, Physica **7**, 817 (1940).

[5] J. R. Pellam, Phys. Rev. **75**, 1183 (1949).

[6] I. M. Khalatnikov, J. Exptl. Theoret. Phys. (U.S.S.R.) **20**, 243 (1950).

[7] J. R. Pellam and C. F. Squire, Phys. Rev. **72**, 1245 (1947).

Chase.[8] In the case of second sound the absorption due to second viscosity should be only of the same order of magnitude as that resulting from the normal fluid viscosity. Thus the total second sound absorption due to viscosity was given by Khalatnikov[6] in 1950 as

$$\alpha_{\text{vis}}=\left(\frac{\omega^2}{2\rho v_2^3}\right)\left(\frac{4}{3}\eta+\zeta_{\text{II}}\right)\frac{\rho_s}{\rho_n}, \tag{3}$$

where ζ_{II} is a second viscosity coefficient.

A more complete analysis of second sound attenuation should include still a third mechanism, namely the loss resulting from diffusive thermal flow within the normal component. Recently (1952) Khalatnikov[9] has extended his theory to include this process, so that finally

$$\alpha=\frac{\omega^2}{2\rho v_2^3}\left[\left(\frac{4}{3}\eta+\zeta_{\text{II}}\right)\frac{\rho_s}{\rho_n}+\frac{K}{C}\right], \tag{4}$$

where the additional term represents this second-order thermal process.[10] Here C is the ordinary specific heat capacity of liquid helium II and K, which is analogous to the ordinary thermal conductivity coefficient, is a parameter deduced from the theory on the basis of the same arbitrary constants employed for computing the viscosity coefficients. Although this second-order thermal flow has no appreciable effect on first sound absorption it provides the major contribution to second sound absorption and outweighs the combined effect of first and second viscosity by a factor of roughly two and one-half.

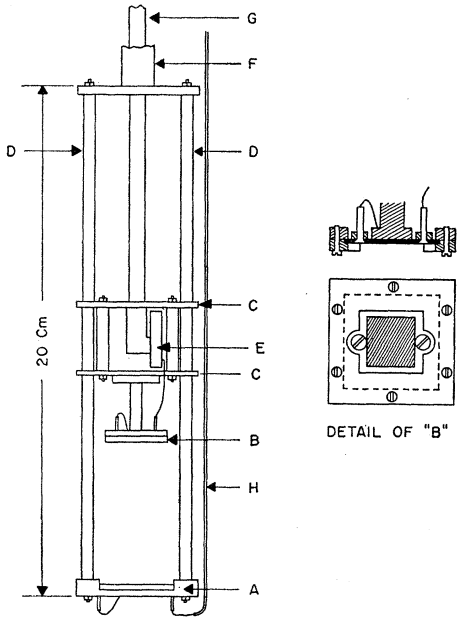

FIG. 1. Second sound cell.

II. EXPERIMENTAL

The frequency range of second sound generation and detection was extended into the submegacycle region during these investigations for two reasons. First, a very high frequency was necessary in order to affect the high wave-preservation properties of these waves sufficiently to produce a measurable attenuation (assuming a frequency squared dependence). Second, in order to preclude possible extraneous losses resulting from interactions between the waves and any containing walls, it was necessary to employ waves of sufficient "directionality" to constitute one-dimensional propagation in the extended medium. Evidently, unless a high order of directionality is attained, the *geometrical attenuation* resulting from beam spreading could actually result in greater pseudoattenuation than that avoided by eliminating constraining walls. It was only necessary, however, to extend the frequencies to sufficiently high values to reduce such geometrical attenuation to an appropriate negligible value. Observations made under such conditions, where geometrical attenuation was effectively outweighed by true attenuation within the second sound wave, presumably gave results associated solely with the properties of the liquid helium II.

a. Second Sound Cell

The geometrical requirements of such a system were satisfied by the configuration represented in Fig. 1. Here the second sound cell is shown consisting of a fixed transmitter A and a movable receiver B. The transmitter A consisted of a thin (0.0005-in.) layer of carbon on a Bakelite backing, to which electrical contact was established in the usual manner with silver paste strip electrodes along two opposite ends of a one-inch square. A square section was used to provide uniform heat flow density throughout the whole wave front. Since the dimensions of this transmitter were always greater than 100 wavelengths of the second sound, an effectively true plane wave of uniform intensity was generated. A cover flange was used to secure the transmitter (and receiver as well) to the flat brass backing plate.

The same type of arrangement was used for the receiver B except that the thickness of the carbon layer was reduced with fine emery paper to increase its thermal response. This receiver, about 1.2 cm on a side, was parallel to the transmitter to within about one thousandth of an inch and maintained its alignment to far greater precision. (This was necessary as the wavelengths were sometimes of the order of only two thousandths of an inch.) Using a receiver of smaller dimensions than the transmitter not only reduced the

[8] K. R. Atkins and C. E. Chase, Proc. Phys. Soc. (London) **A64**, 826 (1951).

[9] I. M. Khalatnikov, J. Exptl. Theoret. Phys. (U.S.S.R.) **23**, 34 (1952).

[10] In 1949 Dingle derived an identical expression for losses due to thermal conduction. By using the value of the heat conductivity coefficient measured for liquid helium I, where the diffusive heat flow is not masked by the internal mass flow, he obtained numerical values of the correct order of magnitude.

alignment problem but also restricted the examination of the second sound beam to the central portions where any fringing or slight beam-spreading tendencies would be least effective. The receiver element was mounted on the frame C which made sliding contact with the four stainless steel alignment rods D. Also mounted on this frame was a small brass compartment E, containing the resistor in series with the receiver and the input circuit to the preamplifier.

The outer Monel tube F provided the mechanical support for the second sound cell and was soldered to the Dewar cap. The inner Monel tube G extended through a packing gland at the top of the Dewar. It provided the means for changing the receiver distance, which could be varied between limits of one-half centimeter and about fifteen centimeters from the transmitter, and also contained the leads to the receiver. The small Monel capillary tube H provided an electrical shield for the input lead to the transmitter.

b. Electronic Equipment

The main experimental problem encountered in the measurements was that of generating and receiving second sound at sufficiently high frequency to provide an observable attenuation. Following this the problem was primarily one of reducing the electrical "cross talk" inherent in such a continuous-wave method to a magnitude that would not obscure the received second sound signals.

The system is represented in the block diagram of Fig. 2. The input frequency $\nu/2$ leading to the transmitter A originated in a crystal oscillator because the frequency ν of the second sound (the input frequency is doubled since heating occurs during *both* halves of the electrical cycle) had to be sufficiently stable to remain in the approximately four cycle per second pass band of the wave analyzer. Although there could be no electrical shielding between the transmitter and receiver, the problem of cross talk was largely self-eliminated by the inherent filter properties of the second sound system. That is, the receiver system was tuned to detect signals at twice the driving voltage frequencies, so that direct electrical pickup of the original frequency did not occur. Electrical cross talk could occur only as the result of anharmonicity in the driving voltage, since the receiver circuit was necessarily tuned to this second harmonic.

In order to prevent this component in the driving voltage from reaching the transmitter, two tuned high-Q filter circuits were inserted directly following the amplifier. These filters discriminated against the second harmonic before the voltage was impressed across the resistance R of the transmitter. In spite of these precautions, enough cross talk occurred at second sound frequencies to complicate the measurement procedure.

The temperature-sensitive resistor R_2 comprising the receiver formed part of a bolometer circuit in which the

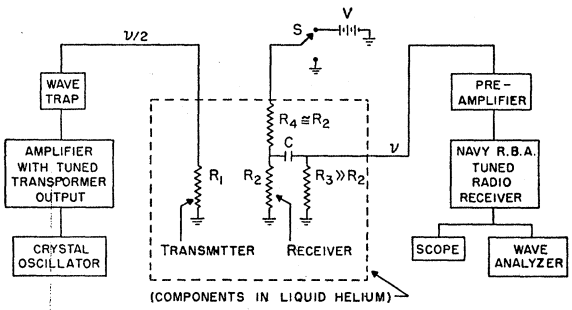

FIG. 2. Block diagram.

bias voltage could be switched off in order to observe the cross talk. In order to improve the signal-to-noise ratio the input circuit to the first stage of amplification was placed in the liquid helium. The received signal at frequency ν was then further amplified and detected by means of a radio receiver delivering an output signal at one kilocycle per second to the wave analyzer. This receiving unit was capable of measuring electrical signals of the order of a few millimicrovolts.

c. Measuring Technique

The technique employed for these measurements involved essentially a free travelling-wave system. This was achieved in practice by operating at sufficiently high second-sound frequencies, and with sufficient transmitter-receiver separation, that the wave attenuation effectively precluded multiple reflections. In this manner certain of the desirable features of both the continuous-wave and the pulse methods were realized. That is, the narrow-band characteristics of this continuous-wave technique provided high receiver sensitivity, while the self-annihilation of the waves provided as effective a distinction between direct and multiply reflected waves as is customarily accomplished with pulses by "separation in time." The method required only that measurements be carried out within the narrow operating range within which direct signals were observable, but multiple reflections eliminated.

This requirement could be met most satisfactorily by recording data at a series of fixed receiver positions, making use of the dependence of second-sound velocity on temperature for controlling the phase relationship between the true second-sound signal and the cross talk. For any particular receiver location, the input power was adjusted to a suitable level to provide observable signals at that position. The receiver sensitivity being maintained constant throughout for a given frequency, the observed signals of the entire series were then reducible to "constant-input data" and plotted on an arbitrary scale. The steps in this process are illustrated in Figs. 3, 4, and 5.

At a given receiver position the continuous wave was turned on and the temperature of the liquid helium II was allowed to increase slowly, while the signal dis-

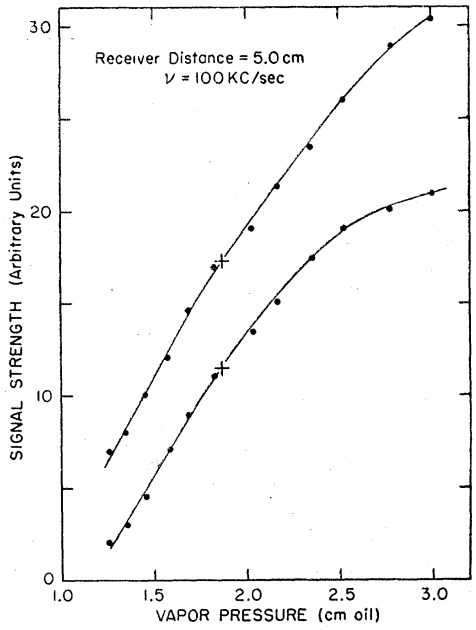

FIG. 3. Received signal plotted *versus* helium vapor pressure at a fixed receiver distance of 5.0 cm, showing maximum and minimum curves which occur as a result of the presence of cross talk. The increase in the curve separation at higher temperature shows the effect also of multiple reflections as the attenuation becomes less.

played on the wave analyzer was recorded as a function of the helium vapor pressure (temperature). These readings consisted of a series of maxima and minima as shown in Fig. 3, depending upon whether the phase of the second sound upon arrival at the receiver coincided with (or opposed) that of the cross talk. For any given receiver position the signal produced by cross talk was

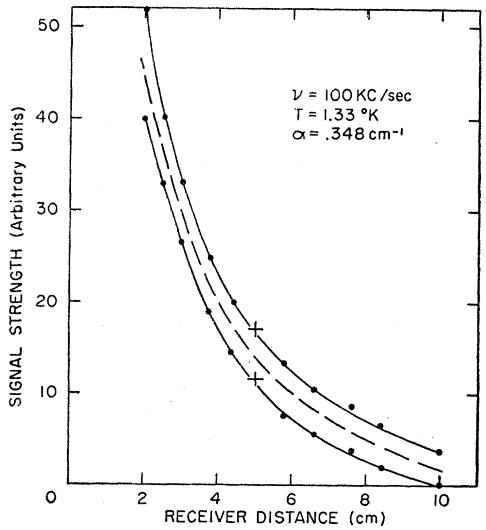

FIG. 4. Received signal strength plotted *versus* transmitter-receiver separation. The dashed curve is taken to represent the true second sound amplitude with cross talk and weakly reflected signals averaged out.

independent of temperature and could be read directly by bypassing the bolometer dc voltage source. Accordingly any spreading in the separation between the maxima and minima was evidence of multiple reflections between the transmitter and receiver. This is illustrated in Fig. 3, where the excess separation between maxima and minima at the higher temperatures, for which the attenuation is less, indicates the arrival of "second-trip waves" at the receiver. The effects of such "second-trip waves" may be recognized in this manner and were usually eliminated by suitable frequency-distance combinations. In any case, their presence in small proportion to the primary wave served only to increase the fluctuations without affecting the mean value.

During a run a set of such curves (as in Fig. 3) were taken at different receiver distances but with constant receiver sensitivity. The attenuation was then evaluated by replotting maxima and minima, as a function of the distances employed, for each of several chosen temperatures. An example is shown in Fig. 4, where the data are plotted for a temperature of 1.33°K, the points being taken from the smooth curves represented by Fig. 3. Finally the dashed curve in Fig. 4 is taken to represent the actual second sound amplitude as a function of distance with the cross talk averaged out.

Replotted on a semilog basis, a straight-line dependence is obtained (the central curve corresponds to the dashed curve of Fig. 4). This behavior of the final data appears to substantiate the reliability of the general method, including the procedure for nullifying the effects of multiple reflections. The consistency of the data in this connection is illustrated by the results given in Fig. 5. For example, the signal strengths plotted at value 10 on the arbitrary scale used here have been sufficiently attenuated beneath the value at the transmitter (zero distance) that the first echo, after two additional transits, would arrive at the receiver attenuated to one or two percent of the primary signal. Consistency of the observed slopes, however, for points both above and below such a value show the negligible effects due to reflections.

d. Extraneous Attenuation

Various precautions were taken to insure that all the observed signal diminution with distance was attributable to true liquid attenuation rather than to any effects associated with the equipment or the geometry.[11] For example, it has been mentioned earlier that the second sound waves were "beamed" in order to avoid the effects of any constraining tube walls. The transmitter, which was one inch square, was centered within a dewar of about $2\frac{3}{4}$ inches inside diameter, thus allowing nearly one inch of liquid between the second

[11] Geometrical and other effects can easily overshadow the true liquid attenuation of second sound. This was evidently the case in an early investigation near the λ point by one of the authors (see reference 5) in which values exceeding the present ones were observed. A realization of the need for measurements free of such possible effects instigated the present research.

sound beam and the nearest wall (except for the guide rods). Attenuation effects due to wall losses were thus eliminated for all practical purposes.

Under these conditions losses resulting from beam spreading were undoubtedly the most serious factor encountered. For order of magnitude, one can consider the angle of spreading to equal the ratio of wavelength to transmitter dimension, so that this effect would be most important at the lower frequencies and in the region where the velocity is highest. For example, at a frequency of 100 kc/sec, and for the maximum wave velocity (about 20 meters/sec), the wavelength λ becomes about $\frac{1}{5}$ millimeter. For the transmitter width (a) of 25 mm, a spreading angle $\theta=\lambda/a$ of 0.008 radian represented the upper limit. Simple geometrical considerations lead to the coefficient of attenuation due to geometry,

$$\alpha_{\text{geom}}=2\theta/a=2\lambda/a^2, \tag{5}$$

for small-angle spreading (where one remembers that the coefficient of power attenuation is twice the coefficient of amplitude attenuation). We thus obtain for the maximum geometrical attenuation $\alpha_{\text{geom}}=0.006$ for the case of worst spreading (or $\log_{10}\alpha_{\text{geom}}/\omega^2=-13.8$).

By comparison, the minimum value of α measured in this region was about 0.11 cm^{-1}, or about twenty times the amount of the attenuation due to spreading. Usually this geometrical attenuation amounted to less than one or two percent of the true liquid attenuation, which was somewhat less than the experimental scatter. Actually the presence of this extraneous attenuation would tend always to increase the measured value but by an amount insufficient to warrant corrections.

III. RESULTS

a. Amplitude Dependence

In Fig. 6 the attenuation is plotted *versus* amplitude for a temperature of 1.38°K and for a frequency of 100 kc/sec. Within the range shown, which includes all amplitudes employed for these experiments, the attenuation is *evidently completely independent of amplitude.* Actually the magnitudes of heat current density (and associated temperature amplitude) which are given represent upper limits to the true values. That is, at the high frequencies employed it is likely that a considerable fraction of the rf heat component was dissipated in the carbon layer and did not contribute to the second sound amplitude; i.e., the bulk carbon could not follow the rapid temperature fluctuations but only a thin layer at the surface. This situation was considered primarily responsible for the rapid decrease in signal strength as frequency was increased; although signals were observed at frequencies as high as 350 kc/sec, the signal strength was not large enough to permit meaningful measurements. Accordingly, the values along the abscissa of Fig. 6 exceed the true magnitudes by the amount of such generator losses at 100 kc/sec.

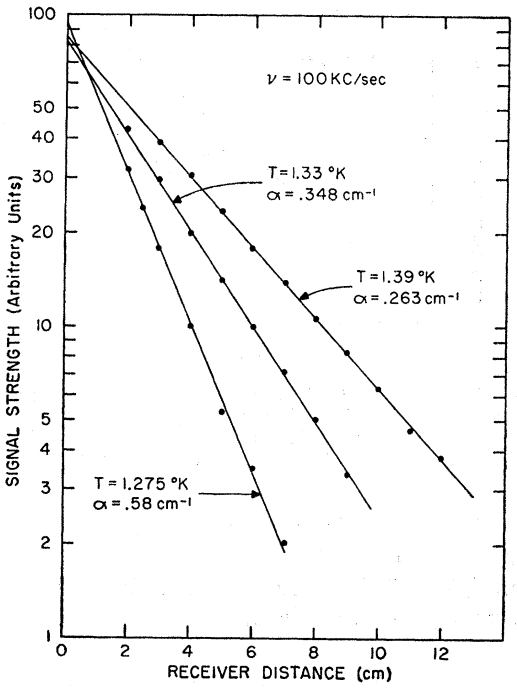

FIG. 5. Semilog plot of second sound amplitude *versus* receiver distance. The attenuation coefficient is equal to the negative of the slope of the straight lines. The rapid variation of attenuation with temperature in this region is evident.

Some recent work by Atkins and Hart[12] (employing the pulse method at a carrier frequency of the order of 20 kc/sec) has been published while this paper was being written, and they report that attenuation does increase with amplitude. This observation was very likely the result of working at sufficiently high heat-current levels that nonlinear effects were important (their amplitudes were much greater[13] than those used in the present work). Such nonlinear effects required an

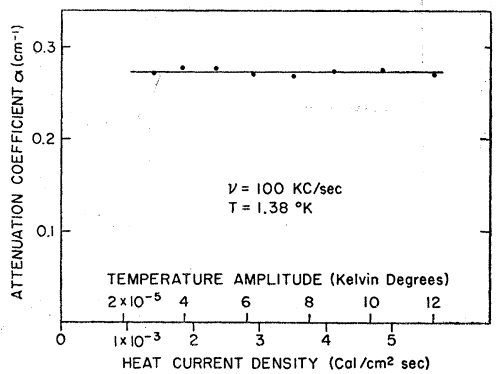

FIG. 6. Plot demonstrates independence of second sound attenuation on temperature amplitude for the amplitude range used in these experiments. Abscissa values represent upper limits to the actual temperature amplitudes.

[12] K. R. Atkins and K. H. Hart, Phys. Rev. **92**, 204 (1953).
[13] K. R. Atkins (private communication).

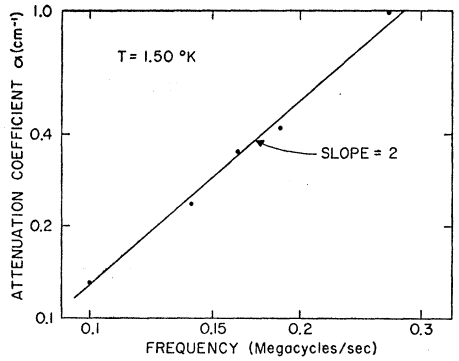

FIG. 7. Log-log plot of attenuation *versus* frequency at a temperature of 1.5°K. The plotted points lie quite well along the straight line which has a slope of 2.0, giving quantitative confirmation of the predicted frequency-squared dependence.

extrapolation of their data toward zero input power in order to obtain results representing the linear region assumed by Khalatnikov and to which the present measurements were confined.

b. Frequency Dependence

As may be seen from the theory, the attenuation of second sound should vary as the square of the frequency; according to Khalatnikov this dependence should obtain, in the temperature interval covered, up to a frequency of about 100 Mc/sec. The measured values of attenuation reported here give quantitative confirmation of this frequency squared behavior.[14] This

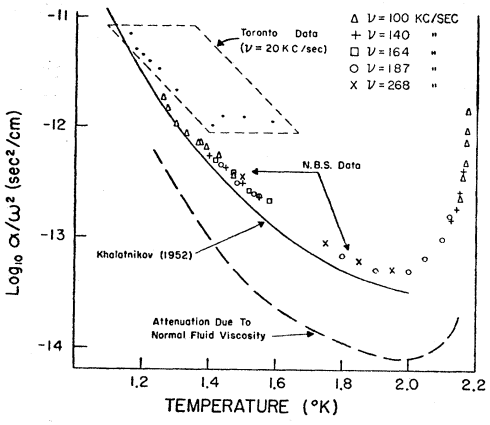

FIG. 8. Semilog plot of α/ω^2 *versus* temperature. Frequencies ($\nu=\omega/2\pi$) at which measurements were made are designated by the various symbols as indicated.

[14] The low-frequency measurements of Atkins and Hart suggest a similar behavior. Their published data were given only at 20 kc/sec, but they remark "at 10 kc/sec and 30 kc/sec it was more difficult to evaluate the beam spreading correction, but the results indicate the small attenuation varies approximately as the square of the frequency." It is not clear, in view of the difficult beam-spreading corrections, to what extent these small attenuations verify the law.

is illustrated for a temperature of 1.5°K in Fig. 7, where α is plotted *versus* frequency on a log-log scale and the straight line has been drawn in with a slope of two. Although data are given here for but a single temperature, the general validity of the relationship is demonstrated in Fig. 8, where α/ω^2 is plotted as a function of temperature for a composite set of frequencies. The internal consistency shown by these data could logically exist, within the range of frequencies employed, only by strict conformity to the frequency-squared law.

c. Temperature Dependence

In Fig. 8 the quantity α/ω^2 is plotted *versus* temperature. Data taken at the various frequencies employed are indicated by different symbols, and the composite curve formed by these points represents a unique, frequency-independent relationship. It will be observed that no data occur within roughly one-tenth of a degree

TABLE I. Attenuation values taken from smooth curve drawn through the experimental points (curve not shown on Fig. 8).

Temperature (°K)	$\alpha/\omega^2\times10^{13}$ (sec²/cm)	Temperature (°K)	$\alpha/\omega^2\times10^{13}$ (sec²/cm)
1.275	14.1	1.80	0.72
1.30	11.2	1.85	0.59
1.35	7.9	1.90	0.51
1.40	5.6	1.95	0.49
1.45	4.25	2.00	0.51
1.50	3.10	2.05	0.66
1.55	2.35	2.10	1.00
1.60	1.82	2.125	1.45
1.65	1.41	2.15	2.51
1.70	1.10	2.16	4.0
1.75	0.89	2.17	8.9

on either side of 1.65°K. As explained earlier, the measurement technique utilized the variation of second sound velocity with temperature, and this gap occurs in the region where second sound velocity is a maximum. The trend of the results is quite clear, however, throughout the entire temperature range from 1.25°K to 2.17°K. The coherence of the data obviated the need for a connecting smooth curve drawn through the points, but values taken from such a curve are presented for reference in Table I.

The dashed curve of Fig. 8 represents the attenuation to be expected from the normal fluid viscosity as given[5] by expression (2), and employing the values of viscosity coefficient η measured by Hollis-Hallett.[15] This curve follows the trend of the data at all temperatures, but in magnitude actually represents only about one sixth of the total attenuation present.

[15] A. C. Hollis-Hallett, Proc. Roy. Soc. (London) **A210**, 404 (1952).

The solid curve represents Khalatnikov's final (1952) prediction as given by expression (4), adding to expression (2) the dynamic terms both in viscosity ("second viscosity") and thermal conductivity. Actually this latest work of Khalatnikov's was unknown to the authors until after the experiments had been completed. *The agreement with the experimental results is remarkably good both in magnitude and in temperature dependence.* Khalatnikov did not extend the curve above 2.0°K because above this temperature the density of excitations is so high that the ideal gas approximations for the phonons and rotons can no longer be considered valid. The increase predicted[5] on the basis of the decrease in wave velocity (α proportional to $\rho_s/\rho_n v_2^3 \sim 1/v_2$) is apparent, however, in the 2.0°K λ-point range.

The data shown within the parallelogram in the upper left-hand portion of Fig. 8 were reported recently by Atkins and Hart[13] for a frequency of 20 kc/sec. Though they plotted values of α for this frequency on a linear scale, we have for comparative purposes replotted this data on the same $\log_{10}(\alpha/\omega^2)$ basis originally employed by Khalatnikov. At their lowest temperatures the data clearly indicate the rapid rise in attenuation with decreasing temperature predicted by Khalatnikov. Above 1.4°K, however, the effects of the large beam spreading at the low frequency employed[16] become more evident. At 1.6°K for example, the geometrical attenuation is apparently already about six times as large as the true attenuation (based on the present results). As a consequence of these large background effects the scatter of their data becomes comparable (see log plot of Fig. 8) to the true liquid attenuation under investigation. By moving Khalatnikov's curve linearly upward to coincide with their points, they demonstrated good agreement within the range covered. Actually they could have obtained absolute determinations from their data below 1.3°K by subtracting the necessary background correction.

d. Conclusions

(1) The attenuation of second sound has been measured as a function of temperature and frequency in the submegacycle range. (2) The results are found to agree substantially with the predictions of Khalatnikov. (3) The frequency-squared dependence of second sound attenuation has been established quantitatively. (4) No dependence of second sound attenuation on amplitude has been observed at the low-power levels employed for these measurements.

[16] The geometrical spreading increases as $1/\nu$ and the second sound attenuation increases as ν^2; thus the ratio of the magnitudes of the two effects ($\alpha_{true}/\alpha_{geom}$) varies as ν^3. At 100 kc/sec, as opposed to 20 kc/sec, the relative importance of the beam spreading is down by a factor of $(5)^3=125$.

PHYSICAL REVIEW VOLUME 95, NUMBER 2 JULY 15, 1954

Temperature-and-Field Emission of Electrons from Metals*

W. W. DOLAN AND W. P. DYKE
Physics Department, Linfield College, McMinnville, Oregon
(Received April 9, 1954)

Both the current density and the distribution in energy of electrons emitted from metals are calculated for various combinations of temperature, applied surface electric field, and work function. A wider range of those variables than previously achieved is made possible by use of numerical integration. The integrand is the usual function based on the free-electron theory of metals and the wave-mechanical barrier transmission coefficient of Sommerfeld and Bethe which assumes a classical image force and a plane surface. Results, which are presented in graphical form, are consistent with the Fowler-Nordheim field emission equation for low temperatures, and with the Richardson thermionic emission formula at low fields. Predicted emission at temperatures up to 3000°K is compared with cold emission at fields between 10^7 and 10^8 v/cm. A qualitative comparison is made between the present results and previous experiments on the transition between field emission and the vacuum arc.

INTRODUCTION

ELECTRONS are emitted from metals under the action of both temperature and electric field. When the temperature is high and the field is low, the process is thermal emission, which is described by the familiar Richardson equation; the effects of intermediate fields on thermal emission are well known as the Schottky effect. When the field is high and the temperature is low, the process is field emission, described by the Fowler-Nordheim equation; the added effect of intermediate temperature has been considered by several authors, as indicated below.

When both temperature and field are high, the emission process is strongly dependent on both variables and is properly described as neither thermal nor field emission; therefore the descriptive term "temperature-and-field emission," or, in abbreviated form, "*T-F*

* This work was supported by the U. S. Office of Naval Research.